

# MEASUREMENTS OF THE FLOW DISTRIBUTION IN SUBCHANNELS OF A WIRE WRAPPED 37-PIN ROD ASSEMBLY

Seok-Kyu Chang, Dong-Jin Euh, Hae Seob Choi, Hyungmo Km, Dong-Won Lee and Hyeong-Yeon Lee

Korea Atomic Energy Research Institute (KAERI)  
Daedeok-daero 989-11, Yuseong-gu, Daejeon, Republic of Korea  
[skchang@kaeri.re.kr](mailto:skchang@kaeri.re.kr); [djeuh@kaeri.re.kr](mailto:djeuh@kaeri.re.kr); [hschoi@kaeri.re.kr](mailto:hschoi@kaeri.re.kr); [hyungmo@kaeri.re.kr](mailto:hyungmo@kaeri.re.kr);  
[dongwon888@kaeri.re.kr](mailto:dongwon888@kaeri.re.kr); [hylee@kaeri.re.kr](mailto:hylee@kaeri.re.kr)

## ABSTRACT

Hydrodynamic experiments for a wire wrapped 37-pin rod bundle have been performed to provide the data of a flow distribution and pressure losses in subchannels. Diameters of the rod and the spacer wire are 8.0 and 1.0 mm, respectively and the lead length of the wrapped wire is 221.5 mm, where in results  $P/D$  and  $H/D$  are 1.13 and 27.69, respectively. Iso-kinetic sampling technique has been adopted for the measurement of a flow distribution of three types of subchannels. Sampling probes which were specially designed to conserve the shape of a flow area for each type of subchannels have been used. Accurate positioning of a sampling probe at a random measuring subchannel has been established by using a precise motorized 3-D traversing system. Experiments have been performed at the conditions of 20 ~ 115 % of a reference flow rate (5.49 kg/s) and 60 °C at the inlet of the test rig. A flow distribution according to each type of subchannels was identified. Pressure drops at three different subchannels were almost identical and independent of subchannel locations.

## KEYWORDS

Wire wrapped rod bundle, Subchannel, Iso-kinetic sampling method, Pressure loss, Friction factor

## 1. INTRODUCTION

A fuel assembly of the SFR (Sodium-cooled Fast breeder Reactor) type reactor generally has a hexagonal cross-section in which there is a closely pitched triangular array rod bundle. One type of the spacing devices of the pitched array for maintaining the flow passage is a helical wire spacer which are wrapped around each fuel pin helically in axial direction. The configuration of a helical wire spacer guarantees the fuel rods integrity by providing the bundle rigidity, proper spacing between rods and promoting coolant mixing between subchannels, and hence, enhances an overall heat transfer coefficient eventually to meet the design requirements, while in adverse effect, increases pressure drop through the flow channel.

It is important to understand the flow characteristics in such a triangular array wire wrapped rod bundle in a hexagonal duct. Many studies have been conducted related to the thermal-hydraulics of the SFR type reactor in terms of the pressure drop, the friction factors and the flow mixing between subchannels. The key geometric parameters are number of fuel pin, rod diameter, rod pitch and lead length of helical wire. Figure 1 illustrates a schematic of a typical SFR wire wrapped assembly and rod configuration, where there shows three different types of subchannel, i.e., interior, edge and corner subchannel.

Cheng and Todreas [1] have suggested the hydrodynamic models and correlations such as bundle friction factors, subchannel friction factors and mixing parameters for a wire-wrapped LMFBR rod bundle. The subchannel friction factors and the mixing parameters have been developed by considering the geometric effects of each type of subchannels for all flow regions.

Earlier hydrodynamic models have been developed by Novenstern [2] and Rehme [3]. Novenstern [2] has firstly developed a semi-empirical model for the wire-wrapped bundle friction factor correlation adopting an empirical correlation factor which accounted for wire effects on a formulation of a smooth pipe. The empirical correlation factor was determined by correlating the bundle experimental data in the turbulent region. Rehme [3] has suggested a widely used wire-wrapped bundle friction factor as a function of the modified Reynolds number using an effective velocity based on the swirl flow velocity around the rod. The bundle friction factor has been calibrated by using Rehme's own bundle experimental data which were taken in the turbulent region.

Lorenz and Ginsberg [4] have conducted an experimental work for establishing a database of mixing and flow distribution in a 91-pin wire wrapped fuel assembly. They employed an electrolytic tracer for mixing measurements and iso-kinetic sampling technique for sampling flow measurements. Cheng [5] has presented constitutive correlations for the analysis of a wire wrapped rod assembly through a series of hydrodynamic experiments with a 37-pin wire wrapped rod bundle. The iso-kinetic extraction method for measuring subchannel velocity, the pitot-static probe for measuring pressure drop and the salt tracer injection method for estimating the inter-channel mixing were used in these experiments.

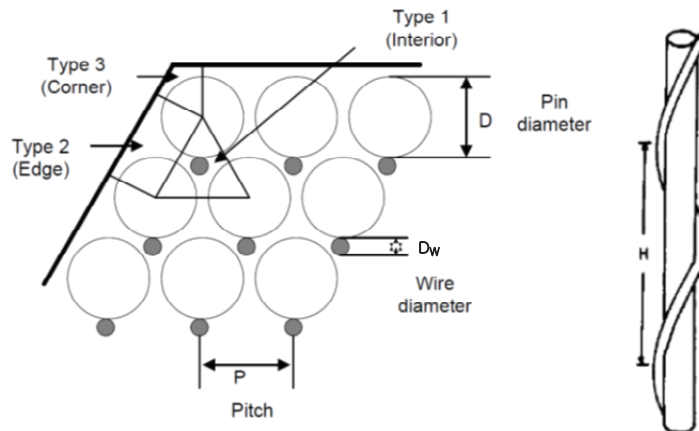


**Figure 1. Configuration of SFR Wire Wrapped Rod Assembly.**

KAERI (Korean Atomic Energy Research Institute) is performing the development program of the 4<sup>th</sup> generation SFR (Sodium-cooled Fast breeder Reactor) type reactor for the next era power generation. Related to this program, the experimental work has been undertaken to quantify the friction and mixing parameters which characterize the flow distribution in subchannels for the KAERI's own bundle geometric configuration. This work presents the hydrodynamic experimental results for the flow distribution and the pressure drop in subchannels of a 37-pin wire wrapped rod bundle which has been fabricated considering the hydraulic similarity of the reference reactor.

## 2. EXPERIMENTAL WORKS

### 2.1. Test Specifications

It is necessary to perform the specific hydrodynamic tests for the verification of the flow characteristics of developing fuel assembly configuration, and these should be done by keeping geometric and dynamic similarities with the prototype [6]. There have been many hydrodynamic experiments for the above purpose and most were conducted as maintaining the geometric similarities i.e., the ratio of pitch to diameter (P/D) and lead to diameter (H/D) comparing to the prototype reactor with reduced fuel rods from 7 to 217 [7]. Water or air has been used as working fluids instead of liquid metal with the same Reynolds number for keeping dynamic similarity because of easiness of measurements and loop maintenance.

The number of pins in a test fuel assembly has been chosen as 37 in this work. Operating flow conditions in a test fuel assembly are 5.49 kg/s at 60 °C which is equivalent to  $Re \sim 37,100$ . Table I summarizes the geometric specifications and the hydraulic conditions of the test fuel assembly.

**Table I. Geometric specifications and hydraulic conditions of 37-pin test assembly**

Geometric Specifications		Hydraulic Conditions	
Rod Dia., D (mm)	8.0	Inlet Press. (MPa)	0.4
Rod Length, L (mm)	1,500	Inlet Temp. (°C)	60
Wire Dia., DW (mm)	1.0	Fluid Density (kg/m <sup>3</sup> )	983.4
Lead Length, H (mm)	221.5	Dynamic Viscosity (Ns/m <sup>2</sup> )	4.67 x 10 <sup>-4</sup>
P/D	1.13	Re number	3.71 x 10 <sup>4</sup>
H/D	27.69		

Configuration of the 37-pin test assembly is illustrated in Fig. 2. Rods are packed tightly shaping triangular subchannels in a hexagonal housing which has dimensions of 66 and 57.16 mm at vertex to vertex and face to face, respectively. These dimensions reflect +0.7% allowance for 37-pin assemblage in a hexagonal duct, and therefore the rod and the wall pitch are determined as 9.05 and 5.06 mm, respectively.

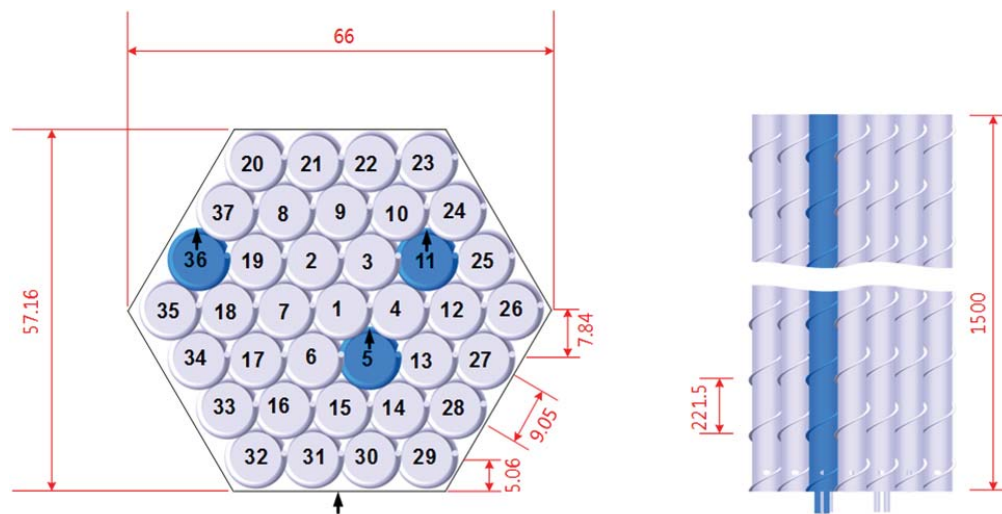


**Figure 2. Configuration of 37-pin Test Fuel Assembly.**

Three special pins i.e., #5, #11 and #36 are for the measurement of the pressure drop through the three-lead distance (664.5 mm) in subchannels. Pin numbers (locations) are typically chosen for the measurements of interior, intermediate and outer subchannels, respectively. The pressure sensing holes are fabricated by penetrating the surface of the tube perpendicularly as shown in Fig. 3. All instrument tubes of pressure

sensing holes through the inside of the rod tubes are guided outside at the bottom of the bundle housing and connected to the differential pressure transmitters. Additional tap holes are fabricated inside of the housing wall at the the same level of sensing holes of the instrument rods. Sensing directions are indicated with arrows as shown in Fig. 2.

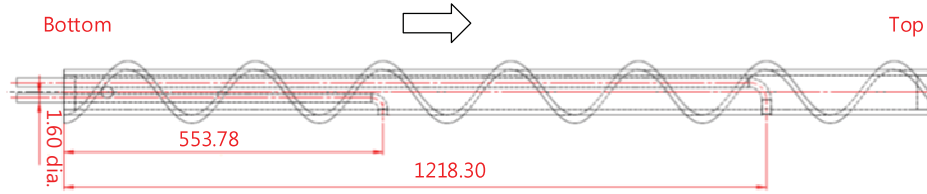


Figure 3. Instrument Rod for the Measurement of Subchannel Pressure Drop.

## 2.2. Experimental Facility

Hydrodynamic tests for the flow distribution and the pressure drop in subchannels of a 37-pin wire wrapped rod bundle have been performed at the experimental facility called the name of CTL-II (Cold Test Loop – II) in KAERI site. This facility is used for hydrodynamic experiments of various fluidic components such as any type of rod bundle and flow inventories at near ambient conditions. It consists of a test rig, a water storage tank and a circulation pump. Figure 4 illustrates a schematic of the experimental facility. The test rig contains a 1,500 mm long 37-pin rod bundle in a hexagonal housing. Four inlets are attached at the lower part of the test rig and the honey comb is placed at the inside to straighten the inlet flow. Four outlets are formed at the upper part of the test rig as the same of the lower part.

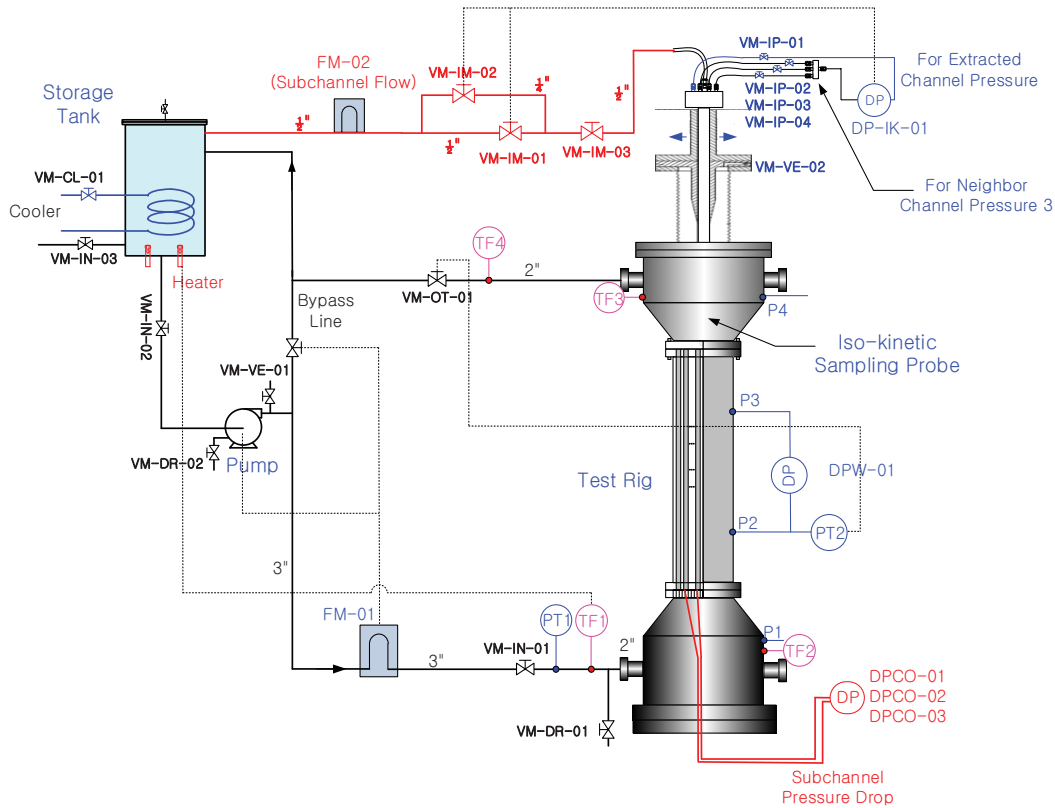


Figure 4. Schematic of the Test Facility.

Loop operating conditions are monitored at the inlet of the test rig from the instruments of mass flow (FM-01), pressure (PT1) and temperature (TF1) and carefully adjusted by controlling the pump speed, the valve opening (VM-OT-01) and the heater power. Experiments have been performed mostly under the loop operating conditions of 5.49 kg/s, ~0.4 MPa and 60 °C at the inlet of the test rig.

Figure 5 illustrates the component of the test rig and the installation of a sampling probe on top of the test rig. The test rig comprises four parts i.e., a lower plenum, a hexagonal housing, a glass cylinder and an upper plenum as shown in the left figure. Coolant flow enters the lower plenum through four inlets and stabilized after the straightener. A hexagonal housing contains a 1,500 mm long 37-pin wire wrapped rod bundle. A short glass cylinder is connected to the top of the hexagonal housing. The top end of a 37-pin rod bundle can be visualized through the glass cylinder and therefore, one can confirm the conditions of a rod array and the alignment of a sampling probe. Coolant flow returns to the storage tank through four outlets of the upper plenum which is connected on the glass cylinder. Right figure shows the installation of the flow sampling probe on top of the upper plenum using a flexible bellows which allows a probe to move in lateral and vertical directions. Sampling flow goes to a mass flowmeter (FM-02) and is measured when an iso-kinetic condition is established at the exit of the measuring subchannel.

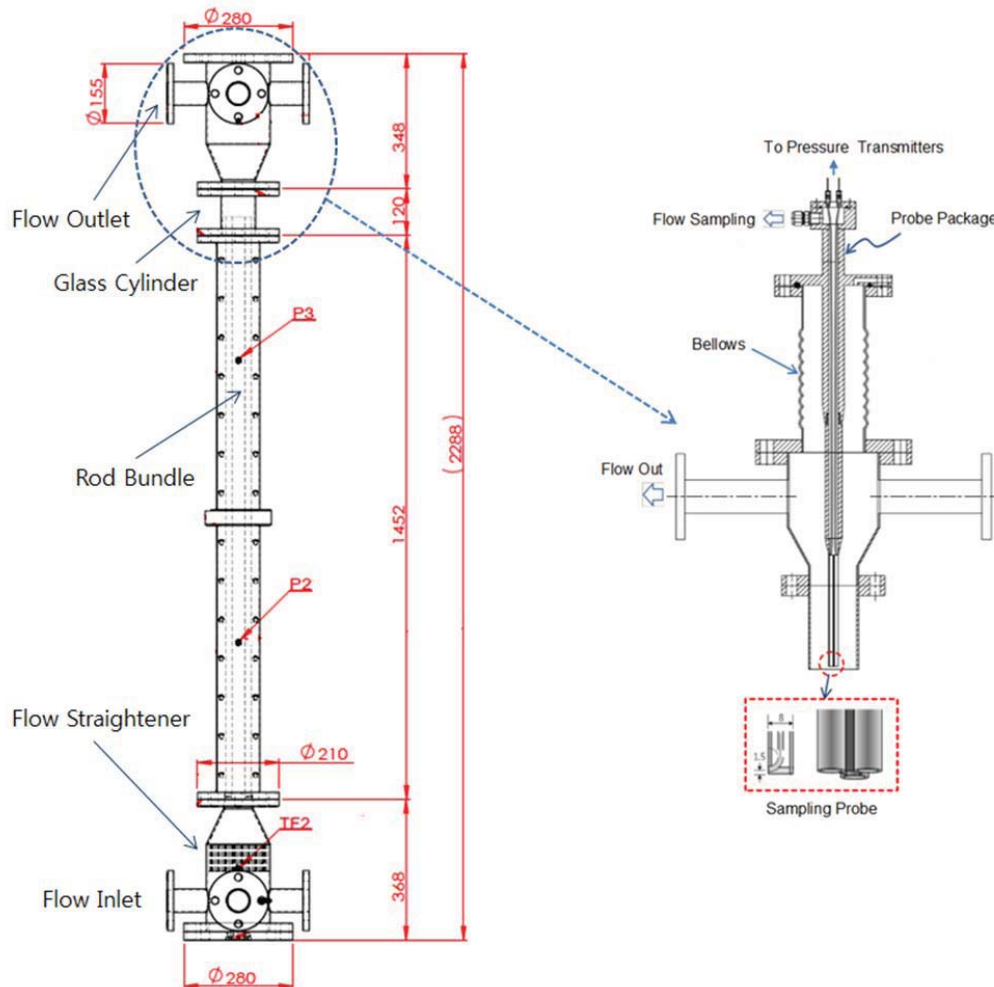


Figure 5. Schematic of the Test Rig.

### 2.3. Experimental Method

The iso-kinetic sampling technique is widely known as a traditional measurement method for the flow rate of subchannels in a rod bundle.

Lorenz and Ginsberg [4] used a 50.8 mm height bare rod arrayed flow divider on a wire wrapped rod bundle. A sampling device was inserted at a particular subchannel and the sampling flow was measured under iso-kinetic condition. To implement iso-kinetic sampling, pressure taps were fabricated at a distance of 1.58 mm from the top end of every rod walls of interest. The edge subchannel taps were located at the same level in a duct wall.

Cheng [5] adopted simple devices such as triangular and rectangular tubes for sampling the flow from the interior and the edge subchannel, respectively. There were pitot tubes and a pressure tap for surrounding pressures and the subchannel inside at device walls to make iso-kinetic conditions. Sampling device was positioned apart some distance from the top of the rod to ensure the stabilized flow getting out from the fluctuating region beyond rod ends.

In this work, the sampling probe was designed in a way that the cross section of the entrance of the sampling probe coincides with the shape of the measuring subchannel. Therefore, three kinds of sampling probe were fabricated for each three types of subchannel. Figure 6 demonstrates the cross section of the iso-kinetic sampling probes which were designed to preserve the flow cross section of three types of subchannels. Sampling probes have pressure taps at 1.5 mm upward from the probe end. For all probes, one inward directed pressure tap is for the measurement of sampling subchannel and the other outward directed taps are for the surrounding subchannels.

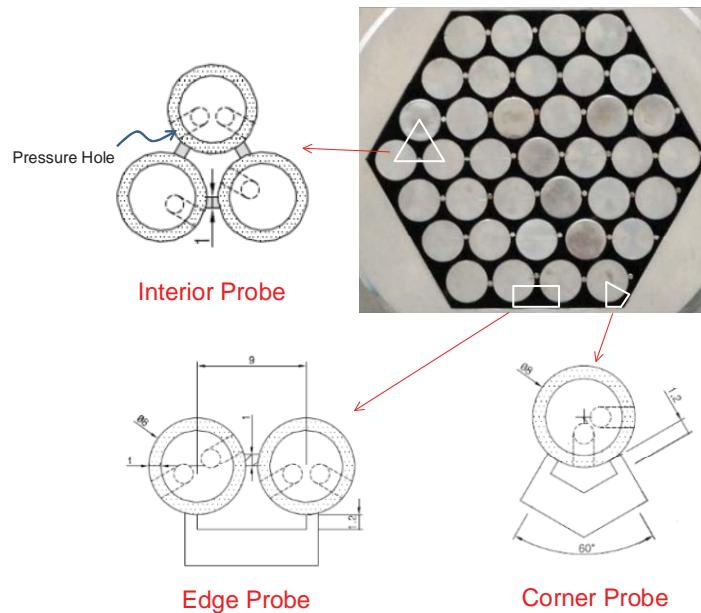


**Figure 6. Cross section of Iso-kinetic Sampling Probes.**

The iso-kinetic condition is considered to be established from the same static pressure ( $DP_{iso-k} \sim 0$ ) as expressed Eq. (1) between the sampling subchannel and the surrounding subchannels by adjusting the sampling flow rate. In an actual situation, the tolerance  $\varepsilon$  was inevitably chosen as 0.2 kPa considering a compromise between the sensitivity of a sampling flow and the stability of a pressure difference.

$$\left| \frac{1}{N} \sum P_{outward} - P_{inward} \right| = DP_{iso-k} < \varepsilon \quad (1)$$

Figure 7 shows the experimental setup of the flow measurement and the pressure drop in subchannels for a wire wrapped 37-pin rod bundle. A motorized 3-D traversing system is adopted to move the iso-kinetic sampling probe accurately to any specified subchannel on the top of the 37-pin rod bundle. A cylindrical view window is equipped at the region of the flow sampling of subchannels for ensuring the accurate probe alignment on the sampling subchannel. The flow sampling line from the probe is connected to the flow control valve (VM-IM-01~03) and the mass flow meter (FM-02). The pressure sensing lines of the sampling and surrounding subchannels are connected to the pressure transmitters (DP-IK-01) to compare the pressure differences. The pressure sensing lines for the measurement of the pressure loss in subchannels are guided outside through the lower plenum and connected to the pressure transmitters (DPCO-01~03).

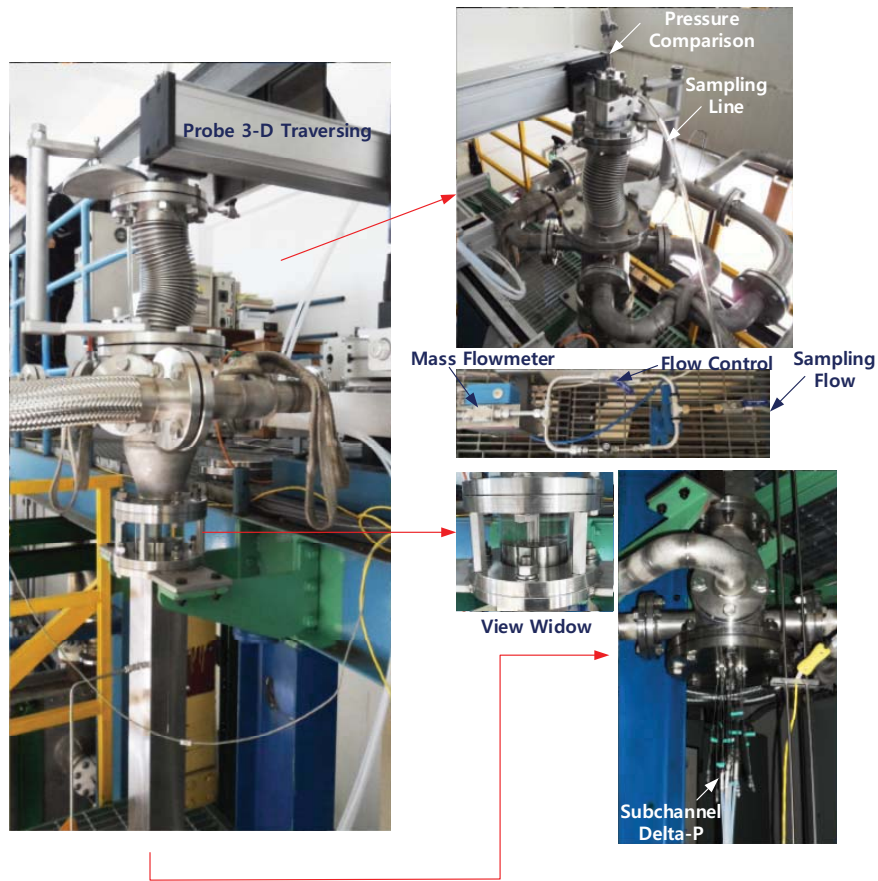


**Figure 7. Experimental Setup of the Test Rig.**

Data acquisition system has been constructed to obtain the experimental data for the flow distribution and the pressure losses in subchannels as well as controlling the loop operating conditions i.e., the main flow rate (FM-01), the loop temperature (TF1) and the system pressure (PF1). Total twelve signals, i.e., four temperatures, two static pressures, four differential pressures and two flow rates were acquired from the signal processor (Hewlett Packard 34970A) with sampling rate of 1 Hz. Acquired data was processed by in house HMI software which had been programed with HP-VEE and stored in a form of ASCII file.

### 3. EXPERIMENTAL RESULTS

The loop operating conditions were maintained with the specified experimental conditions during the hydrodynamic tests. The inlet temperature of a test rig was sustained at constant (60 °C or 40 °C) using the heater and cooler in a water storage tank. The specified main flow rate from 20% to 115% of a reference flow rate (5.49 kg/s) was controlled by keeping a constant speed of the circulation pump. The system pressure at the inlet of a test rig was also stably maintained at the range of roughly from 0.2 to 0.5 MPa according to the main flow rate.

Prior to the execution of the main experiments, CFD analysis had been performed to verify relevance of the developed measuring method and the working range of instruments. Used analysis tool was a commercial CFD code, 'STAR-CCM+' [8]. Complete test rig with a 37-pin rod bundle containing upper and lower plenum was modelled with 45 million computational cells for the accurate and effective calculation, and the anisotropic  $k-\epsilon$  model was used for the turbulence model. It was confirmed that the sizing and the instrumentation of the test facility had been properly designed. The CFD results were also utilized for comparisons of the analysis and the experimental data of the flow distribution and the pressure drop in subchannels.

Figure 8 demonstrates the locations and the identifications of the measured subchannels for the sampling flow rate and the pressure loss. The iso-kinetic sampling flow rate has been measured at 42 subchannels which are described their locations and the identification numbers in the figure. All corner and edge subchannels have been measured on a 37-pin rod bundle. Eighteen interior subchannels have been measured at symmetrically selected locations as shown.

The pressure loss in subchannels at three-lead flow distance has been measured at subchannel #3, #31, #71 and #65 from the fabricated pressure sensing holes at pin #5, #11, #36 and the housing wall, respectively.

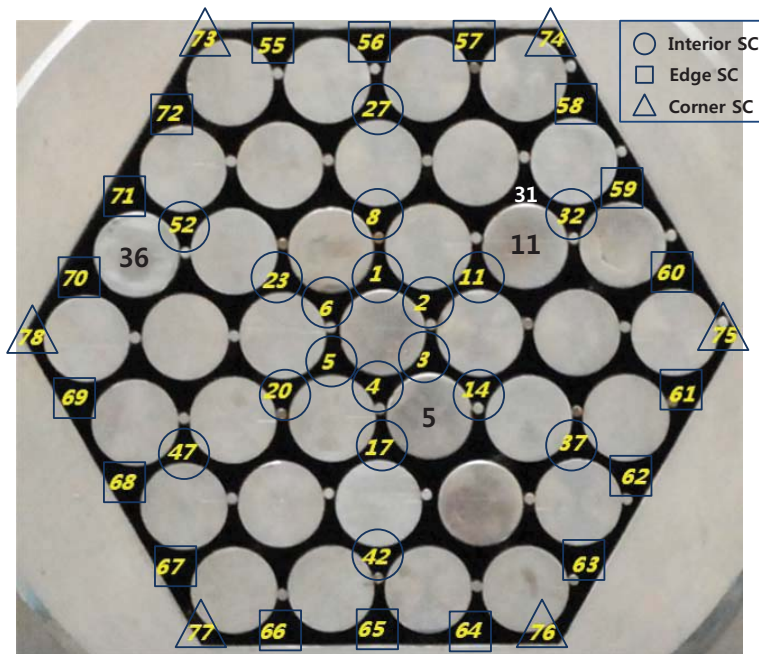


**Figure 8. Locations and Identifications of Subchannels for the Iso-kinetic Sampling Test.**

### 3.1. Flow Distribution in Subchannels

Measurements of the sampling flow rate for each type of subchannels have been performed under the isokinetic condition. For the type of the interior subchannel, eighteen subchannels have been selected considering the geometrical symmetry, where all six subchannels for first ring, one third i.e., six subchannels for second ring and one fifth i.e., also six subchannels for third ring. The sampling flow rates for these interior subchannels have been measured using the specific sampling probe for the interior subchannel (refer Figure 6).

Figure 9 shows the sampling flow rates for interior subchannels at eighteen locations in a 37-pin rod bundle. The flow conditions were 20 ~ 115% of a reference flow rate (5.49 kg/s) and 60 °C (40 °C for one case) at the inlet of the test rig. A case of 100% flow rate at 40 °C has the same Reynolds number with a case of 72.2% flow rate at 60 °C. Standard deviations of the measurements are indicated with error bars. It was observed that the flow rates at inner subchannels (1<sup>st</sup> ring) are slightly higher than the flow rates at outer subchannels (3<sup>rd</sup> ring). This is caused by differences of the flow area between inner subchannels and outer subchannels, where the flow area of the inner subchannels tends to be larger than that of the outer subchannels which are confined to the hexagonal housing, under the free (not fixed) conditions of all rods at exit side. The flow deviations at the same ring were also observed because of differences of the flow area at each subchannel caused by free locations of rod ends.

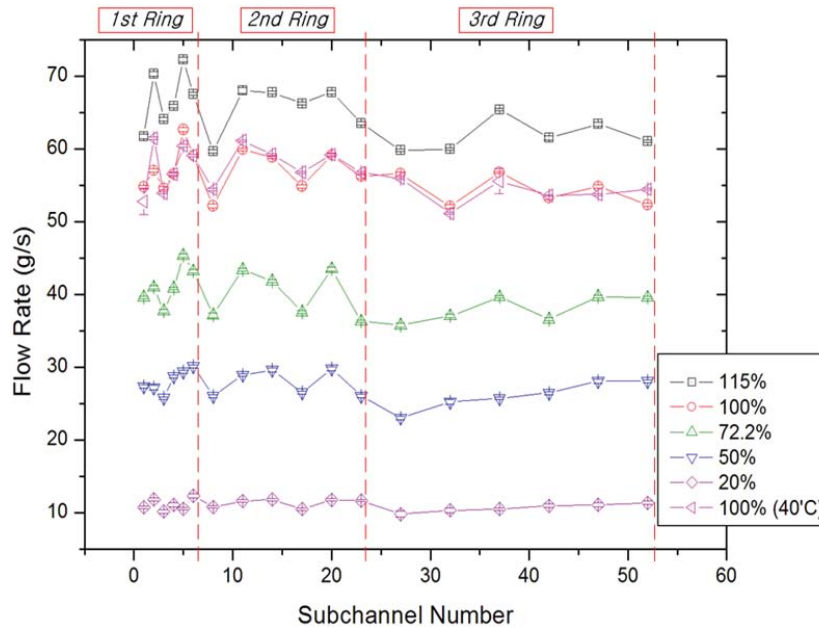


**Figure 9. Sampling Flow Rates in Interior Subchannels.**

Other types of subchannel i.e., the edge and the corner subchannels have been measured for all subchannels in a 37-pin rod bundle (eighteen edge and six corner subchannels). The specific sampling probes were used for the measurements of the edge and the corner subchannels, respectively (refer Figure 6). The flow conditions were a reference flow rate (5.49 kg/s) and 60 °C at the inlet of the test rig. Including the results of the interior subchannels, Figure 10 shows the sampling flow rates at a reference flow rate for all types of subchannels at 42 locations in a 37-pin rod bundle. The flow rates at the edge subchannels were higher than those at the interior subchannels because of the larger flow area and lower friction loss due to the smooth wall at the inside of the hexagonal duct. The lowest flow rates were occurred at the corner subchannels and it was caused by the smallest flow area. The flow deviations at the edge subchannels and the corner subchannels were also observed and were deduced from the slight

variations of the flow area at subchannels caused by the free rod ends. Error bars indicate the total uncertainties including the random and the systematic uncertainties of the sampling flow rates in this figure.

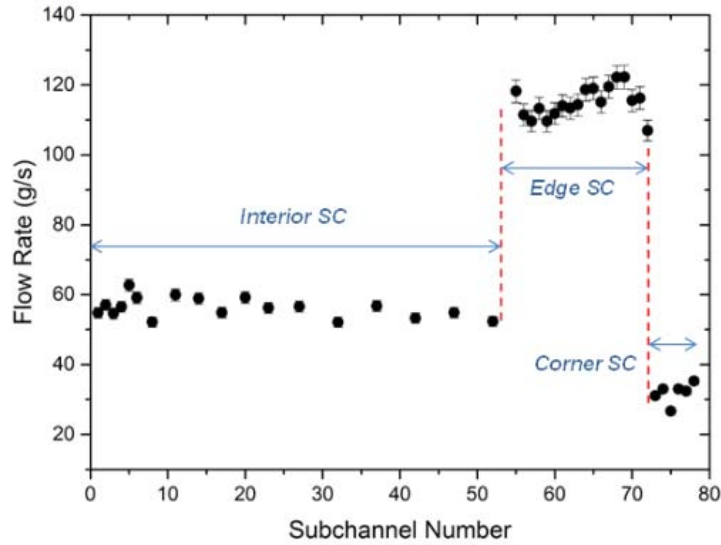


**Figure 10. Subchannel Flow Distribution in a 37-pin Rod Bundle at a Nominal Flow Condition.**

### 3.2. Pressure Loss in Subchannels

The pressure loss in subchannels have been measured for three-lead flow distance (664.5 mm) at subchannel #3, #31 #71 and #65 as described in Figure 3. The data of subchannel #3 was not included in this figure because of the fabrication defect of the pressure sensing hole.

The pressure losses in all measured subchannels were almost identical regardless of whether the subchannel locations are under the same flow condition as shown in Figure 11.

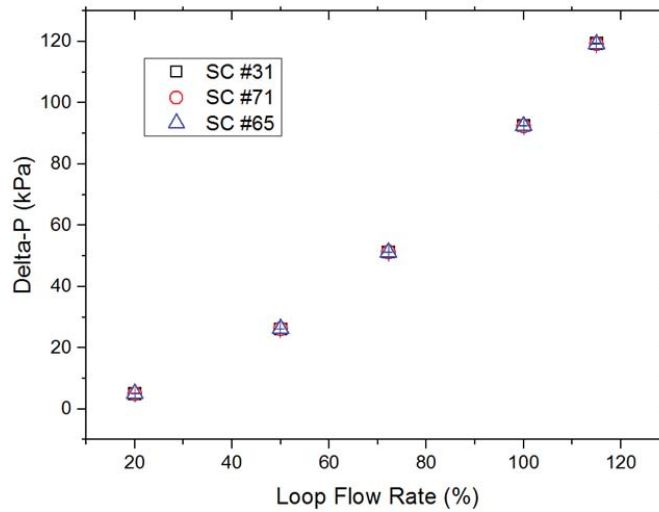


**Figure 11. Pressure Losses in Subchannels (100% = 5.49 kg/s).**

This should be obvious since variations in pressure among subchannels at the entrance of the rod bundle would lead to redistribute the flow rate and a resolution of the pressure discrepancies. Eventually, the lateral pressure distribution in a rod bundle is almost flat at upstream of the developed region. Novenstern model [2] is one of the well-known traditional friction factor correlations for the wire wrapped fuel assembly. This model has been estimated with the above measured data in a case of the interior subchannel. CFD result for the pressure loss in subchannels has been also compared with the pressure loss data.

Figure 12 presents the comparisons of the correlation and the CFD result with the experimental data. As shown, Novenstern correlation predicted the pressure drop in subchannels very well while the CFD analysis slightly under-predicted, when comparing to the measured data of the nominal flow condition.

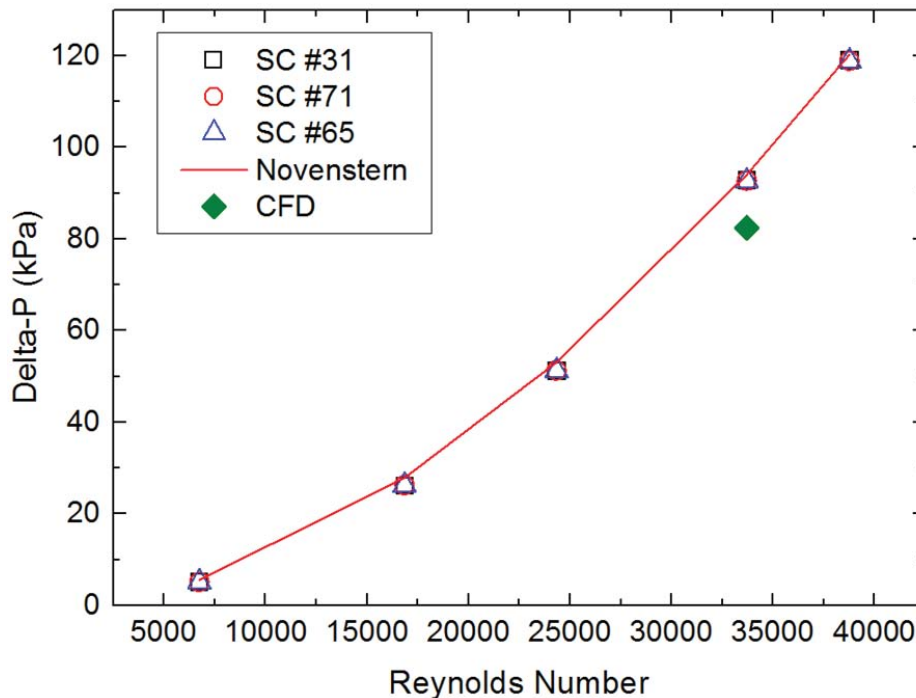


**Figure 12. Comparison of the Experimental Data and Predictions for the Pressure Losses in Subchannels.**

#### 4. CONCLUSIONS

Hydrodynamic experiments for a 37-pin wire wrapped test assembly has been performed to provide the data of a flow distribution and pressure losses in subchannels for verifying the analysis capability of subchannel analysis codes for a KAERI's own prototype SFR reactor.

Iso-kinetic flow sampling technique has been adopted to measure the flow rate at each subchannels. Three type of sampling probes have been specially designed to conserve the shape of the flow area for each type of subchannels. Sampling probes were moved and accurately aligned at any measuring subchannel by using a precise motorized 3-D traversing system.

All of the edge and the corner subchannels including the symmetrically chosen eighteen interior subchannels have been measured to identify the characteristics of the flow distribution in a 37-pin rod assembly.

Pressure drops at the interior and the edge subchannels have been also measured to recognize the friction losses of each type of subchannels.

Most have been performed at the experimental conditions of 20 ~ 115 % of reference flow rate (5.49 kg/s) and 60°C (equivalent to  $Re \sim 37,100$ ) at the inlet of the test rig.

The flow rates at the edge subchannels were higher than those at the interior subchannels because of the larger flow area and lower frictional loss, while the lowest flow rates were occurred at the corner subchannels due to the smallest flow area.

The pressure loss data in three measured subchannels were almost identical whatever the subchannel locations are, under the same flow condition. The prediction by Novenstern correlation was well agreed with the measurement data.

## ACKNOWLEDGMENTS

The authors would like to thank the National Research Foundation of Korea (NRF) grant funded by the Korea Government (MEST) (No. 2012M2A8A2025638).

## REFERENCES

1. S.K. Cheng and N.E. Todreas, "Hydrodynamics Models and Correlations for Bare and Wire-Wrapped Hexagonal Rod Bundle – Bundle Friction Factors, Subchannel Friction Factors and Mixing Parameters," *Nuclear Engineering and Design*, **92**, pp. 227-251 (1986).
2. E.H. Novenstern, "Turbulent Flow Pressure Drop Model for Fuel Rod Assemblies Utilizing a Helical Wire-wrap Spacer System," *Nuclear Engineering and Design*, **22**, pp. 19-27 (1972).
3. K. Rehme, "Pressure Drop Correlations for Fuel Element Spacers," *Nuclear Technology*, **17**, pp. 15-23 (1973).
4. J.J. Lorenz and T. Ginsberg, "Coolant Mixing and Subchannel Velocities in an LMFBR Fuel Assembly," *Nuclear Engineering and Design*, **40**, pp. 315-326 (1977).
5. S.K. Cheng, "Constitutive Correlations for Wire-wrapped Subchannel Analysis under Forced and Mixed Convection Conditions," Ph.D. Thesis (1984).
6. G. Hetsroni, "Use of Hydraulic Models in Nuclear Reactor Design," *Nuclear Science Engineering*, **28**, 1 (1967).
7. S.R. Choi, "Test Requirements of Experiments for SFR Thermal-hydraulic Characteristics," SFR-CD250-TR-01-2011 Rev.00, KAERI (2012).
8. CD-adapco, 'STAR-CCM+' Code Manual, Ver.7.06, CD-adapco (2011).